International Journal Of
Industrial Electronics Control and Optimization
Print ISSN: 3517-2645
Online ISSN: 3568-2645
Homepage: https://ieco.usb.ac.ir/

An Impedance-Based Approach for Locating Short-Circuit Faults in Inverter-Based Active Distribution Networks

Morteza Behbahanipour[1] | Seyed Fariborz Zarei[1] | Mohammadhadi Shateri[2]

Department of Electrical and Computer Engineering, Qom University of Technology, Qom, Iran.[1]
Département de génie des systèmes, École de technologie supérieure, Université du Québec, Montréal, Canada.[2]
Corresponding author's email: zarei@qut.ac.ir

Article Info

Article type:
Research Article

Article history:
Received: 17-May-2024
Received in revised form: 27-June-2024
Accepted: 30-June-2024
Published online: 02-July-2024

Keywords:
Active distribution network,
Fault location,
Impedance-based approach,
Inverter-based distributed generation resources.

ABSTRACT

This paper proposes an impedance-based approach for locating short-circuit faults in active distribution networks (DNs). This topic is a crucial task for operators, especially in grids with inverter-based distributed generators (IBDGs). Various methods have been proposed in this research area, including traveling waves, impedance-based methods, and artificial intelligence (AI) techniques. Among them, the impedance-based scheme offers a straightforward and efficient feature suitable for integration with AI-based techniques. This paper introduces an enhanced fault localization method based on impedance estimation, consisting of two main components: (i) fault distance determination and (ii) faulty section identification. This method accounts for the modeling of inverter-based resources under both symmetrical and asymmetrical faults, incorporating the impact and behavior of such sources. Unlike conventional impedance-based methods, our approach does not require network information such as structure, lines, load data, or voltage and current measurements along the feeder at multiple points. It can serve as a feature in AI-based techniques, significantly enhancing accuracy and reducing the complexity of such techniques. To validate the efficacy of the proposed approach, we conducted a series of time-domain case studies and provided mathematical proofs. The results demonstrate the effectiveness of our scheme in accurately locating faults with varying resistances at different positions in the presence of IBDGs.

I. Introduction

Accurate fault location is crucial for the efficient operation of power distribution systems as it speeds up the restoration of the affected section and the resumption of faulty line operation. Fault locators are specialized devices designed to detect and pinpoint faults in power distribution systems [1]. Advanced fault locators offer a more reliable and efficient solution for identifying and resolving faults in DNs [2]. In these devices, the core processor, including the fault location scheme, is the key component. The scheme should determine the faulted section and the location of the fault within the section. The several connected feeders of the distribution network, with multiple laterals, complicate the process of fault location. Additionally, the prevalent fault resistance in the distribution network is another influencing factor. Moreover, by connecting inverter-based distributed generations (IBDGs) to the distribution network, the network becomes active with multiple feeding locations. This transformation turns the distribution systems into multi-source systems with dispersed production resources, making fault location more intricate and necessitating further investigation. During short-circuit fault conditions, the control of inverters is crucial in generating output currents. This further complicates the behavior of IBDGs, consequently affecting the fault location to the same degree.

Generally, the existing fault location schemes are divided into three categories of "impedance-based methods", "traveling waves-based schemes" and "artificial-intelligence-based techniques" [3]. Among these, impedance-based methods are preferred due to their simplicity and effectiveness, allowing for straightforward implementation using a simple thresholding model and potential integration as inputs for AI-based techniques.

Consequently, this paper focuses on impedance-based schemes, with a detailed literature review provided subsequently.

Zhu et al. [4] pioneered the impedance iterative method, presenting an iterative approach for single-phase fault analysis and addressing multi-response challenges through current patterns. Lee et al. [5] later enhanced this technique by effectively resolving multi-response issues using flow patterns. Yang et al. [6] utilized the distributed line model to develop an iterative algorithm for single-phase faults, whereas Nouri et al. [7] extended this model to include single-phase and 2-phase fault localization. Works by Salim et al. [8] and Bretas et al. [9] introduced an iterative algorithm to mitigate load change issues, focusing on single-phase fault detection in the presence of DGs, and later incorporated a neural network to tackle multi-response problems [10]. Nunes et al. [11] further refined the algorithm by integrating DGs into fault analysis for single-phase and 3-phase faults. In addition, an iterative method was proposed in [12] & [13] for comprehensive fault location using an equation and addressed multi-response challenges through the current error index. Other works such as [14] & [15] contributed an iterative algorithm for all fault types, considering DGs and employing a 2nd degree equation. In 2021, Dashti et al. [16] introduced an iterative algorithm for all fault scenarios using a 5th degree equation, incorporating DG presence and leveraging artificial intelligence for load estimation, along with pattern matching to resolve multi-response issues. Despite their evolution, these methods vary in their ability to detect specific faults and in their capacity to accommodate DG units or address multi-response issues, especially in scenarios with high fault current patterns. The effectiveness of these methods is influenced by network equipment like reclosers and breakers.

Building upon the foundations established in [17], this work proposes an extended impedance-based fault location method to address the correct performance under all types of faults, support inverter-based distributed generators (DGs), and solve multi-response problems with minimal information. The key contributions and novelties of the proposed method, compared to the existing approaches and the study [17], are as follows:

- A generalized inverter control scheme under both symmetrical and asymmetrical short-circuit faults is modeled in developing the proposed scheme.
- Grid codes for inverter-based resources are considered in the proposed approach.
- Different short-circuit fault conditions are taken into account in the proposed scheme.
- The proposed approach does not rely on network information, and communication infrastructure is not required.
- The proposed scheme effectively identifies the faulted section in a multi-line, multi-lateral distribution network by considering the multi-response problems.

The paper is organized as follows: Section II covers the preliminaries of impedance-based methods, while Section III delves into the behavior of IBDGs under short-circuit fault conditions. The fundamentals of the proposed fault location approach are presented in Section IV, followed by the proposed scheme for identifying the faulty section in Section V. The paper concludes with case studies, simulation results, and conclusions in Sections VI, VII, and VIII, respectively.

II. Preliminaries of the Impedance-Based Methods

Similar to the distance relay logic, impedance-based methods utilize voltage and current phasors to estimate fault impedance. These methods are typically categorized as ‘single head’ or ‘double head’ methods. The ‘single head’ method relies on substation voltage and current data to pinpoint the fault location, while the ‘double head’ method analyzes voltage and current data from both ends of the distribution system to determine the fault location. A visual representation of the impedance-based method is depicted in Fig. 1 using a basic circuit model. Within this model, V_m denotes the voltage at the measurement node, Z_l represents fault impedance per unit length, l indicates the distance of the fault from the measurement node, V_s stands for source voltage, and Z_s signifies source impedance. Equation (1) outlines the interrelation among these parameters, facilitating the calculation of fault distance from the relay point [3] and [18].

$$l = \frac{V_m}{I_f . Z_l} \tag{1}$$

III. Modeling of Inverter-Based Distributed Generations

A. Control Loops

The schematic diagram of Fig. 2 illustrates a grid-connected inverter [19] with its two control loops of an inner current control loop and an outer DC link voltage control loop. This section will focus on the current control scheme under a short-circuit fault condition [20]. The Double Synchronous Reference Frame (DSRF) scheme has been extensively utilized in the literature to discuss the control scheme under fault condition. The DSRF method involves transforming the currents into the “dq” frame using two clockwise and counter-clockwise synchronous reference frames (SRF), as shown in Fig. 3 [21]. In the DSRF scheme, the “dq” components consist of DC and double-frequency pulsating components. As an example, when utilizing the clockwise-SRF, the positive-sequence component of $iabc$ appears as DC-components and pulsating components with a frequency of double the line frequency (2ω0). Filtering out the pulsating terms results in two independent variables, $Id+$ and $Iq+$, which can be controlled separately. Consequently, Fig. 4 displays the commonly used structure for controlling these variables. The output filter model is represented by $\frac{1}{L_f.s+R_f}$, and $\mathrm{G_i}$ is the current controller, as given in equation (2), where BW is the current control loop bandwidth.

$$\mathrm{G_i(s)} = \mathrm{K_p} + \frac{\mathrm{K_i}}{\mathrm{s}}$$
$$\mathrm{K_p} = \mathrm{BW}.\mathrm{L_f} \tag{2}$$
$$\mathrm{K_i} = \mathrm{BW}.\mathrm{R_f}$$

Due to space constraints, this paper focuses exclusively on the current reference generation under fault condition, and it does not delve into the specifics of the power inverter control system. However, interested readers are encouraged to refer to the related references for further information on topics such as feed-forward compensation and the current control loop decoupling, phase-locked-loop implementation, and DC-link voltage controller [22, 23, 24].

B. Behavior Under Fault Condition

According to the grid codes, the grid-connected inverters are expected to deliver reactive current during short-circuit faults to assist the power grid [25]. This requirement is incorporated in this paper, as depicted in Fig. 5 and detailed in (3).

$$I_{q0-GC} = \begin{cases} -2.5I_n(V_1 - 0.9) & 0.5 < V_1 < 0.9 \\ I_n & V < 0.5_1 \end{cases} \quad (3)$$

In a general form, assume that the grid voltages and the output currents are expressed as shown in (4) and (5), respectively.

$$V = V_1 e^{j\omega t} \quad (4)$$

$$I = I_{d0} e^{j\omega t} + I_{q0} e^{j(\omega t - \frac{\pi}{2})} \quad (5)$$

, where $V1$ is the grid voltage positive sequence component. Also, $Id0$ and $Iq0$ are positive sequence currents aligned with "d" and "q" axes of SRF, respectively.

Substituting (4) and (5) into (6) gives the injected active power flowing into the grid as shown in (7).

$$p(t) = \Re(1.5I^{*}\mathrm{V}) \quad (6)$$

$$\bar{p}(t) = 1.5V_1 I_{d0} \quad (7)$$

Substituting equation (7) into equation (5) and calculating the amplitude of the three-phase currents yields the following equation for three-phase current values.

$$|I_{abc}| = \sqrt{\bar{p}^2 A^2 + I_{q0}^2}, \text{ where } A = \frac{2}{3V_1} \quad (8)$$

This equation specifies the current injected by IBDGs in terms of the bus voltage. The obtained current references are utilized in developing the proposed fault location scheme, which ensures the correct operation in presence of IBDGs.

IV. Fundamentals of the Proposed Fault Location Method

In this section, we will first outline the process for determining the distance of various types of faults along a power line. Subsequently, we will elaborate on how this approach can be adapted to effectively manage networks with IBDGs.

A. Calculation of Fault Distance in a Sample Line

Fig. 6 shows a sample line, which is used for developing the fault distance calculation equations. In this figure, d is fault distance in per unit; m and n are phases "a", "b" or "c"; r , i are real and imaginary parts of variables; V_{sa} is phase "a" terminal "S" voltage; V_{Fm} is phase "m" fault point voltage; I_{Fm} is phase "m" fault current; I_{Lm} is phase "m" load current; I_{sa} is phase "a" sending-end current; I_{sm} is phase "m" sending-end current; R_{Fm} is phase "m" Fault resistance; Z_{aa} is phase "a" self-impedance; Z_{th} is terminal "R" equivalent impedance; V_{th} is terminal "R" equivalent voltage.

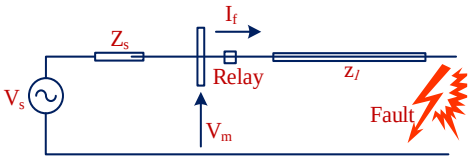

Fig. 1. The concept of impedance-based methods

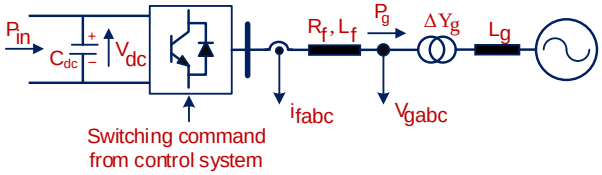

Fig. 2. Schematic diagram and power circuit of a grid-connected inverter

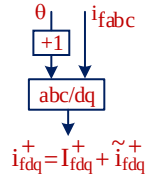

Fig. 3. Obtaining "dq" component using clockwise and counter-clockwise synchronous reference frames (SRFs), namely double-SRF (DSRF)

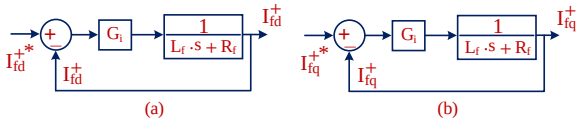

Fig. 4. Control of positive/negative sequence current components of Id +, Iq + in DSRF (a) positive-sequence current control in "d" axis of clockwise SRF, (b) positive-sequence current control in "q" axis of clockwise SRF.

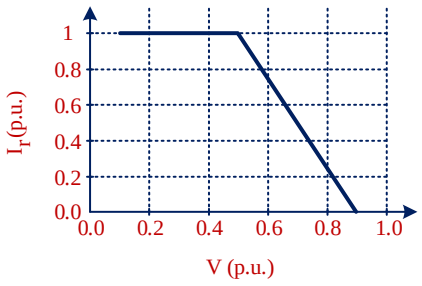

Fig. 5. Reactive current requirement under short circuit fault condition according to the Danish grid code.

With refer to Fig. 6, the steps for calculating the single-phase fault distance in a line are as follows [5], [8]:

1. As an initial assumption, the load current during the fault equals to the load current before the fault.

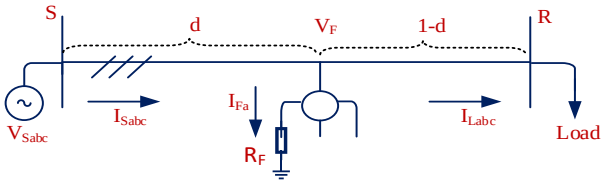

Fig. 6. LG short-circuit fault in a line

2. Calculate the fault current:

$$I_{sm} = I_{Fm} + I_{Lm} \tag{9}$$

3. Calculate the fault distance:

$$\begin{bmatrix} d \\ R_F \end{bmatrix} = \frac{\begin{bmatrix} I_{Fmi} & -I_{Fmr} \\ -M_{2m} & M_{1m} \end{bmatrix}}{M_{1m}I_{Fmi} - M_{2m}I_{Fmr}} \cdot \begin{bmatrix} V_{Smr} \\ V_{Smi} \end{bmatrix} \tag{10}$$

where,

$$M_{1m} = \sum_k (Z_{mkr}I_{Skr} - Z_{mki}I_{Ski})$$
$$M_{2m} = \sum_k (Z_{mkr}I_{Ski} + Z_{mki}I_{Skr}) \tag{11}$$

4. Calculate the fault point voltage:

$$\begin{bmatrix} V_{Fa} \\ V_{Fb} \\ V_{Fc} \end{bmatrix} = \begin{bmatrix} V_{Sa} \\ V_{Sb} \\ V_{Sc} \end{bmatrix} - d. \begin{bmatrix} Z_{aa} & Z_{ab} & Z_{ac} \\ Z_{ba} & Z_{bb} & Z_{bc} \\ Z_{ca} & Z_{cb} & Z_{cc} \end{bmatrix} . \begin{bmatrix} I_{Sa} \\ I_{Sb} \\ I_{Sc} \end{bmatrix} \tag{12}$$

5. Update the load current at the moment of the fault, assuming a constant impedance load.

a- If the estimated fault is downstream of IBDG:

Calculate the paralleling capacity of the loads and lines, and obtain the load current from the opposite equation (refer to Fig. 7). The presence of IBDG affects the voltage and current at the beginning of the line [9][26].

$$I_{Lm} = \frac{V_{Fm}}{Z_{th\,m}} \tag{13}$$

b- If the estimated fault is above IBDG:

Calculate the load current from the opposite equation (refer to Fig. 8). The presence of IBDG affects the load current at the end of the line [11][27].

$$I_{Lm} = \frac{V_{Fm} - V_{th\,m}}{Z_{th\,m}} \tag{14}$$

6. Return to step 2, update the fault current, and repeat the steps until convergence .

$$|d_n - d_{n-1}| < \delta \tag{15}$$

B. *Assessing the Different Types of Faults*

Referring to Fig. 9, Fig. *10*, and Fig. 11, if a two-phase to ground, two-phase, or three-phase fault occurs, the third stage of section A is obtained from the following equations [8]:

a- If a two-phase fault occurs between phases "m" and "n" and the ground

In this case, the following equation is applied.

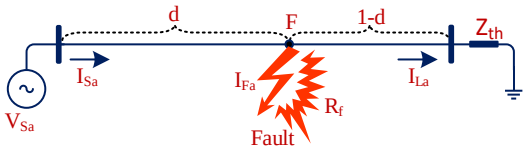

Fig. 7. The fault is downstream of IBDG

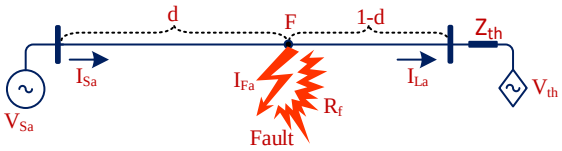

Fig. 8. The fault is upstream of IBDG

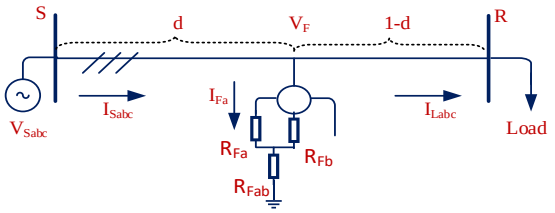

Fig. 9. LLG short-circuit fault in a line

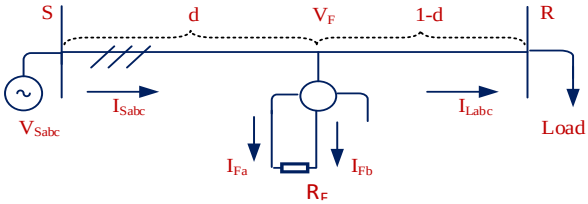

Fig. 10. LL short-circuit fault in a line

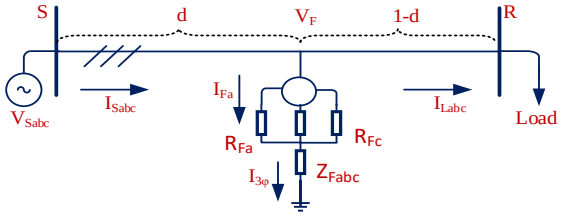

Fig. 11. LLL short-circuit fault in a line

$$\begin{bmatrix} d \\ R_{Fm} \\ R_{Fn} \\ R_{Fmn} \end{bmatrix} = T_1 . \begin{bmatrix} V_{Smr} \\ V_{Smi} \\ V_{Snr} \\ V_{Sni} \end{bmatrix} \tag{16}$$

where,

$$T_1 = \begin{bmatrix} M_{1m} & I_{Fmr} & 0 & I_{Fmr} + I_{Fnr} \\ M_{2m} & I_{Fmi} & 0 & I_{Fmi} + I_{Fni} \\ M_{1n} & 0 & I_{Fnr} & I_{Fmr} + I_{Fnr} \\ M_{2n} & 0 & I_{Fni} & I_{Fmi} + I_{Fni} \end{bmatrix}^{-1}$$

b- If a two-phase fault occurs between phases "m" and "n",

In this case, the following equation is applied.

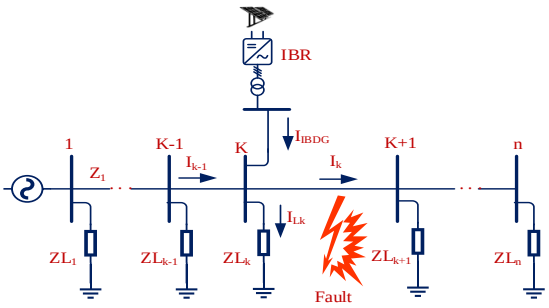

Fig. 12. The distribution network with a fault in downstream of IBDG.

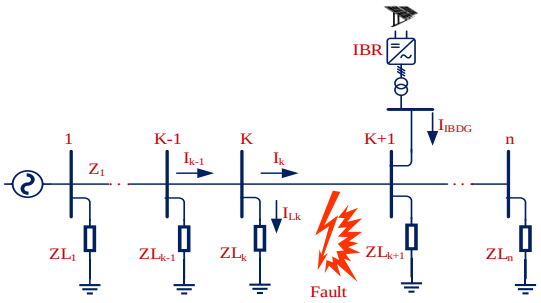

Fig. 13. The distribution network with a fault in upstream of IBDG.

$$\begin{bmatrix} d \\ R_F \end{bmatrix} = \begin{bmatrix} M_3 & I_{Fmr} \\ M_4 & I_{Fmi} \end{bmatrix}^{-1} \cdot \begin{bmatrix} V_{Smr} - V_{Snr} \\ V_{Smi} - V_{Sni} \end{bmatrix} \quad (17)$$

where,

$$M_3 = \sum_k \left((Z_{mkr} - Z_{nki}).I_{Skr} - (Z_{mki} - Z_{nki}).I_{Ski} \right)$$
$$M_4 = \sum_k \left((Z_{mkr} - Z_{nki}).I_{Ski} - (Z_{mki} - Z_{nki}).I_{Skr} \right) \quad (18)$$

where k is phases “a”, “b” or “c”.

c- If a three-phase fault occurs between phases “a” and “b” and c

In this case, the following equation is applied.

$$\begin{bmatrix} d \\ R_{Fa} \\ R_{Fb} \\ R_{Fc} \\ R_{Fabc} \\ X_{Fabc} \end{bmatrix} = T_2 \cdot \begin{bmatrix} V_{Sar} \\ V_{Sai} \\ V_{Sbr} \\ V_{Sbi} \\ V_{Scr} \\ V_{Sci} \end{bmatrix}$$

where,

$$T_2 = \begin{bmatrix} M_{1a} & I_{Far} & 0 & 0 & I_{3\phi r} & -I_{3\phi i} \\ M_{2a} & I_{Fai} & 0 & 0 & I_{3\phi i} & I_{3\phi r} \\ M_{1b} & 0 & I_{Fbr} & 0 & I_{3\phi r} & -I_{3\phi i} \\ M_{2b} & 0 & I_{Fbi} & 0 & I_{3\phi i} & I_{3\phi r} \\ M_{1c} & 0 & 0 & I_{Fcr} & I_{3\phi r} & -I_{3\phi i} \\ M_{2c} & 0 & 0 & I_{Fci} & I_{3\phi i} & I_{3\phi r} \end{bmatrix}^{-1} \quad (19)$$

$$I_{3\phi} = I_{Fa} + I_{Fb} + I_{Fc}$$
$$Z_{Fabc} = R_{Fabc} + JX_{Fabc} \quad (20)$$

$$I_k = I_{k-1} - I_{Lk} + I_{IBDG}$$
$$I_{Lk} = \frac{V_k}{Z_{Lk}}$$
$$V_k = V_{k-1} - L.Z_{k-1}.I_{k-1}$$
$$|I_{IBDG}| = \sqrt{\bar{p}^2 A^2 + I_{q0}^2} \quad (21)$$
$$A = \frac{2}{3V_k}$$

C. *Extending the Equations to the Network*

In cases where the calculated distance "d" along a line exceeds 1.0, it becomes necessary to apply the distance algorithm for the subsequent line. This iterative process is continued until a "d" value less than one is obtained for at least one line. In this specific scenario, faults occurring in sections A or B are assumed to arise within a network incorporating distributed generation resources. As outlined in section A, determining the distance along each line necessitates knowledge of the voltage and current at the line's origin, as well as the load specifications at the line's terminus.

a- If the estimated fault is downstream of IBDG

The voltage and current at the beginning of the faulted line are derived from the equations presented below:

where,

V_k	voltage vector at k[th] node
Z_k	impedance matrix of k[th] line section
Z_{Lk}	impedance of k[th] load
I_k	current vector of k[th] line section
I_{Lk}	current vector of k[th] load
L	line length

The equations given in (21) consist of the equation (8) which was obtained in section III . Also, I_{IBDG} is the current injected by IBDG. The voltage vector at k-th node can be obtained through a power flow program [28], as shown in Fig. 12.

b- If the estimated fault is above IBDG,

The voltage and current at the beginning of the faulted line are obtained from the following equations, knowing the structure of Fig. 13:

$$I_k = I_{k-1} - I_{Lk}$$
$$I_{Lk} = \frac{V_k}{Z_{Lk}} \quad (22)$$
$$V_k = V_{k-1} - L.Z_{k-1}.I_{k-1}$$

V. The Proposed Method to Identify the Faulty Section

In distribution networks, impedance-based techniques can encounter challenges due to multiple potential solutions arising from various sub-branches. To address this issue, this section adopts an approach in which each solution identified in Section IV is treated as a potential fault location. Subsequently, a fault index is computed for each potential location. The fault location

with the lowest index value is then determined as the most accurate fault location. This methodology aids in pinpointing the precise fault location amidst the complexities of distribution networks [12].

A. Single Phase Fault

According to Fig. 6, if a fault occurs in phase "a", the values of healthy phases "b" and "c" are incorporated into the equation presented below.

$$E_{index} = |I_{Fb}|^2 + |I_{Fc}|^2 \quad (23)$$

B. Double Phase Line-to-Line Fault

According to Fig. 9 and Fig. 10, if a two-phase fault occurs between phases "b" and "c", the values from the healthy phase "a" are incorporated into the equation presented below.

$$E_{index} = |I_{Fa}|^2 \quad (24)$$

C. Three Phase Fault

According to Fig. 11, in the event of a three-phase fault occurring between phases "a", "b" and "c", the equation presented below is employed [13]:

$$E_{index} = |I_{Fa,act} - I_{Fa}|^2 + |I_{Fb,act} - I_{Fb}|^2 + |I_{Fc,act} - I_{Fc}|^2 \quad (25)$$

From the calculated value of I_F in (1), the actual fault currents in all of the phases are computed by steady-state fault analysis. Let the actual fault currents be $I_{Fa,act}$, $I_{Fb,act}$, $I_{Fc,act}$. The error index is then defined as in equation (25).

The flowchart depicted in Fig. 14 illustrates the fault location process outlined in this study. Initially, relays detect the fault, followed by the sampling of voltage and current signals. The fault type is then determined based on these signals, which leads to the implementation of a fault location algorithm. Further details of this process are elaborated upon below.

- *Pre-Fault Analysis*

The pre-fault analysis involves calculating the voltage and current of subsequent buses step-by-step from one bus to another, using the initial feeder's pre-fault voltage and current. By considering the power consumption of loads (S_{LK}) and applying specific equations, the load impedance prior to the fault is determined. It is assumed that this load impedance remains constant both pre and post-fault.

$$I_{LK} = \left(\frac{S_{LK}}{V_k}\right)^* \qquad Z_{LK} = \frac{V_k}{I_{Lk}} \quad (26)$$

- *Post-Fault Analysis*

In the post-fault analysis, the impedance of loads from the previous step is utilized along with voltage and current measurements after the fault to calculate the values at the start of each line. Kirchhoff's laws and ladder power flow analysis are employed for this calculation. Subsequently, the distance algorithm for each line, illustrated in Fig. 14, is executed based on the obtained voltage and current values.

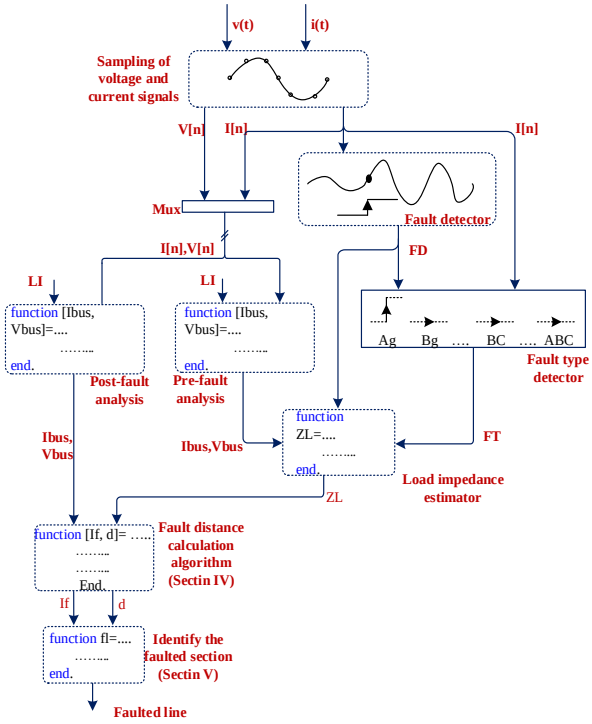

Fig. 14. Flowchart of the proposed method

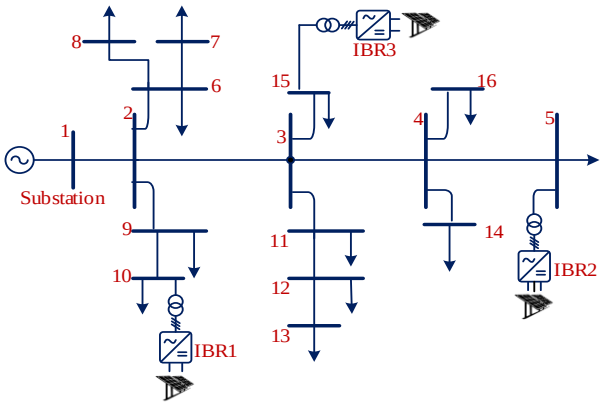

Fig. 15. Single line diagram of test system

VI. Case Study

Fig. 15 presents the single-line-diagram of a three-phase, 11 kV, 50 Hz modified IEEE 15-bus radial distribution system [29]. The line parameters and load data for the 15-bus radial distribution system are sourced from [30]. In this model, three inverter-based distributed generators (IBDGs), which are photovoltaic inverters, are integrated at bus-5, bus-10, and bus-15.

To evaluate the performance of the proposed fault location method, the modified 15-bus distribution feeder was simulated using detailed time-domain simulation in the MATLAB/Simulink environment. The system includes 14 line sections, 16 buses, 12 load buses, and three inverter based generators. The system has a total three-phase power of 7.5 MVA, with each of the inverter based distributed generators

TABLE I. LOAD DATA OF TEST SYSTEM

node	active power (kW)	reactive power (kVar)
1	0	0
2	44.1	44.99
3	70.1	71.44
4	40	142.82
5	44.1	44.99
6	140	142.82
7	140	142.82
8	70	71.414
9	70	71.44
10	44.1	44.99
11	140	142.82
12	70	71.414
13	44.1	44.99
14	70	71.414
15	44.1	44.99

TABLE II. LINE DATA OF TEST SYSTEM

Line No.	from	to	*r* (ohm)	*x* (ohm)
1	1	2	1.35309	1.32349
2	2	3	1.17024	1.14464
3	3	4	0.84111	0.82271
4	4	5	1.52348	1.0276
5	2	9	2.01317	1.3279
6	9	10	1.68671	1.1377
7	2	6	2.55727	1.7249
8	6	7	1.0882	0.734
9	6	8	1.25143	0.8441
10	3	11	1.79553	1.2111
11	11	12	2.44845	1.6515
12	12	13	2.01317	1.3579
13	3	15	1.52348	1.0276
14	4	14	2.23081	1.5047
15	4	16	1.9702	0.8074

TABLE III. THE ACCURACY OF THE FAULT DISTANCE CALCULATION METHOD

R_F (Ω)	Error [%]		
	LG	*LL*	*3PH*
0	0.01	0.00	0.01
10	0.01	0.02	0.01
20	0.03	0.03	0.04
50	0.08	0.09	0.06
100	0.20	0.22	0.24

TABLE IV. THE ACCURACY OF IDENTIFYING THE FAULTY SECTION

Actual value of d and faulty section	feeder 1-2		feeder 2-3		feeder 2-6	
	d	*EI* *	*d*	*EI*	*d*	*EI*
0.2 feeder 2-3	1.37	----	0.200	8.96* e-9	0.127	1.23
0.5 feeder 2-6	1.26	----	0.775	2.59	0.500	6.88* e-8
0.8 feeder 2-9	1.54	----	.·961	1.95	0.635	2.75

* EI: Error Index

contributing 250 KVA. The IBDGs operates at an output voltage of 250 V, and are connected to the network via a transformer.

To validate the methodology, a four-wire grounded neutral RL model was employed. The feeder configuration exhibits unequal distances between phases and non-transposed lines, resulting in an unbalanced line impedance matrix. The line impedance matrix was generated using Carson's equations [31]. Load and line information is detailed in the table I and II.

VII. Simulation Results

In this section, we present the outcomes of tests conducted on fault conditions at various distances from the feeder's origin. These faults encompass single-phase, two-phase, and three-phase scenarios. The findings are detailed in Tables III and IV. Table III showcases the fault distance calculations in the distribution grid with the inclusion of IBDG. The table illustrates that as the fault's phase count and resistance increase, the method's precision diminishes. Nonetheless, even under the most challenging circumstances, the proposed approach maintains high accuracy. Table IV presents the results of fault section determination. When the fault distance 'd' is smaller than faults detected in multiple lines, there are several potential fault locations. According to this table, the faulty section is accurately identified from the potential fault sites, effectively resolving the issue of multiple possible answers.

The percentage errors were calculated by (27):

$$\text{error } (\%) = \left| \frac{d_{actual} - d_{estimated}}{L_T^{\square}} \right| \times 100 \qquad (27)$$

where $d_{estimated}$ is the estimated fault distance in km, d_{actual} is the real fault distance in km, and $L_T^{\square}$ is the total line length in km.

VIII. CONCLUSION

This paper examines various existing fault location methods, highlighting their principles and fundamentals. To address the limitations of these methods, an enhanced feature based on impedance-based methodology is proposed, requiring only local terminal data. This approach overcomes the challenges of traditional impedance-based methods, which include the necessity for extensive system and load data, voltage and current measurements, and knowledge of the distribution system structure. To evaluate the performance of the proposed scheme, a series of equations and mathematical proofs are developed for SLG, LL, LLG, and LLL short-circuit faults. These proofs demonstrate the accuracy and effectiveness of the new method. To further validate its performance, extensive time-domain simulations are conducted using a modified 15-bus IEEE network with multiple branches and inverter-based DGs, including photovoltaic systems and type IV wind generators.

The accuracy of the fault distance calculation method is assessed for LG, LL, LLG, and LLL faults at various distances from the network's substation and across different feeders. The results show that the distance calculation error is minimal, with a worst-case scenario error of 0.24% for different fault resistances ranging from 0 to 100 Ohms.

In addition, the accuracy of the faulty section detection method is evaluated for all identified faults. A specific error index is proposed and computed for each potential fault, ensuring that the faulty section is identified without any errors.

In conclusion, the proposed methodology is suitable for distribution systems with multiple laterals and both balanced and

unbalanced loads, even in the presence of inverter-based DGs under faults with different resistances at various locations. This method offers high accuracy compared to traditional techniques for fault location. Additionally, the proposed feature can be integrated into AI-based techniques, significantly improving accuracy and simplifying complexity.

REFERENCES

[1] Yadegar, M., Zarei, S. F., Meskin, N., & Blaabjerg, F. (2023). A Distributed High-Impedance Fault Detection and Protection Scheme in DC Microgrids. IEEE Transactions on Power Delivery.

[2] Stefanidou-Voziki, P., Sapountzoglou, N., Raison, B., Dominguez Garcia, J.L.: A review of fault location and classification methods in distribution grids. Electr. Power Syst. Res. 209, 108031 (2022).

[3] S. Gururajapathy, H. Mokhlis, and H. Illias, "Fault location and detection techniques in power distribution systems with distributed generation: A review," Renewable and Sustainable Energy Reviews, vol. 74, pp. 949-958, 2017.

[4] Jun Zhu, D. L. Lubkeman and A. A. Girgis, "Automated fault location and diagnosis on electric power distribution feeders," in IEEE Transactions on Power Delivery, vol. 12, no. 2, pp. 801-809, April 1997, doi: 10.1109/61.584379.

[5] Seung-Jae Lee et al., "An intelligent and efficient fault location and diagnosis scheme for radial distribution systems," in IEEE Transactions on Power Delivery, vol. 19, no. 2, pp. 524-532, April 2004, doi: 10.1109/TPWRD.2003.820431.

[6] X. Yang, M. Choi, S. Lee, C. Ten and S. Lim, "Fault Location for Underground Power Cable Using Distributed Parameter Approach," in IEEE Transactions on Power Systems, vol. 23, no. 4, pp. 1809-1816, Nov. 2008, doi: 10.1109/TPWRS.2008.2002289.

[7] H. Nouri and M. M. Alamuti, "Comprehensive Distribution Network Fault Location Using the Distributed Parameter Model," in IEEE Transactions on Power Delivery, vol. 26, no. 4, pp. 2154-2162, Oct. 2011, doi: 10.1109/TPWRD.2011.2161620.

[8] R. H. Salim, M. Resener, A. D. Filomena, K. R. C. De Oliveira, and A. S. Bretas, "Extended fault-location formulation for power distribution systems," *IEEE Transactions on Power Delivery*, vol. 24, no. 2, pp. 508-516, 2009.

[9] A. S. Bretas and R. H. Salim, "Fault Location in Unbalanced DG Systems using the Positive Sequence Apparent Impedance," 2006 IEEE/PES Transmission & Distribution Conference and Exposition: Latin America, 2006, pp. 1-6, doi: 10.1109/TDCLA.2006.311611.

[10] R. H. Salim, K. R. C. de Oliveira, A. D. Filomena, M. Resener and A. S. Bretas, "Hybrid Fault Diagnosis Scheme Implementation for Power Distribution Systems Automation," in IEEE Transactions on Power Delivery, vol. 23, no. 4, pp. 1846-1856, Oct. 2008, doi: 10.1109/TPWRD.2008.917919.

[11] J. U. N. Nunes and A. S. Bretas, "Impedance-based fault location formulation for unbalanced primary distribution systems with distributed generation," 2010 International Conference on Power System Technology, 2010, pp. 1-7, doi: 10.1109/POWERCON.2010.5666589.

[12] K. Ramar and E. E. Ngu, "A new impedance-based fault location method for radial distribution systems," IEEE PES General Meeting, Minneapolis, MN, USA, 2010, pp. 1-9, doi: 10.1109/PES.2010.5588189.

[13] R. Krishnathevar and E. E. Ngu, "Generalized Impedance-Based Fault Location for Distribution Systems," in IEEE Transactions on Power Delivery, vol. 27, no. 1, pp. 449-451, Jan. 2012, doi: 10.1109/TPWRD.2011.2170773.

[14] S. F. Alwash, V. K. Ramachandaramurthy and N. Mithulananthan, "Fault-Location Scheme for Power Distribution System with Distributed Generation," in IEEE Transactions on Power Delivery, vol. 30, no. 3, pp. 1187-1195, June 2015, doi: 10.1109/TPWRD.2014.2372045

[15] F.M. Aboshady, D.W.P. Thomas, Mark Sumner, A new single end wideband impedance based fault location scheme for distribution systems, Electric Power Systems Research, Volume 173, 2019, Pages 263-270, ISSN 0378-7796, https://doi.org/10.1016/j.epsr.2019.04.034

[16] H. Mirshekali, R. Dashti, A. Keshavarz, A. J. Torabi and H. R. Shaker, "A Novel Fault Location Methodology for Smart Distribution Networks," in IEEE Transactions on Smart Grid, vol. 12, no. 2, pp. 1277-1288, March 2021, doi: 10.1109/TSG.2020.3031400.

[17] Morteza Behbahani poor, and Seyed Fariborz Zarei, "A Fault Location Scheme for Distribution Networks with Inverter-Based Resources," presented at the POWER ELECTRONICS AND DRIVES: SYSTEMS AND TECHNOLOGIES CONFERENCE PEDSTC. 2024, [Online]. Available: https://sid.ir/paper/1132495/en

[18] Zarei, Seyed Fariborz, Hossein Mokhtari, and Frede Blaabjerg. "Fault detection and protection strategy for islanded inverter-based microgrids." IEEE Journal of Emerging and Selected Topics in Power Electronics 9.1 (2019): 472-484.

[19] Zarei, Seyed Fariborz, Mohamad Amin Ghasemi, and Saeed Khankalantary. "Current limiting strategy for grid-connected inverters under asymmetrical short circuit faults." International Journal of Electrical Power & Energy Systems 131 (2021): 107020.

[20] D. Tzelepis, A. O. Rousis, A. Dyśko, C. Booth, and G. Strbac, "A new fault-ride-through strategy for MTDC networks incorporating wind farms and modular multi-level converters," International Journal of Electrical Power & Energy Systems, vol. 92, pp. 104- 113, 2017.

[21] Du, Y. Liu, G. Wang, P. Sun, H.-M. Tai, and L. Zhou, "Three?phase grid voltage synchronization using sinusoidal amplitude integrator in synchronous reference frame," International Journal of Electrical Power & Energy Systems, vol. 64, pp. 861-872, 2015.

[22] A. Yazdani and R. Iravani, Voltage-sourced converters in power systems: modeling, control, and applications: John Wiley & Sons, 2010.

[23] F. Blaabjerg, R. Teodorescu, M. Liserre, and A. V. Timbus, "Overview of control and grid synchronization for distributed power generation systems," IEEE Transactions on industrial electronics, vol. 53, no. 5, pp. 1398-1409, 2006.

[24] R. Teodorescu, M. Liserre, and P. Rodriguez, Grid converters for photovoltaic and wind power systems vol. 29: John Wiley & Sons, 2011.

[25] J. Jia, G. Yang, and A. H. Nielsen, "A review on grid-connected converter control for short-circuit power provision under grid unbalanced faults," IEEE Transactions on Power Delivery, vol. 33, no. 2, pp. 649-661, 2017.

[26] Zarei, Seyed Fariborz, et al. "A Fault Detection Scheme for Islanded-Microgrid with Grid-Forming Inverters." 2021 6th IEEE Workshop on the Electronic Grid (eGRID). IEEE, 2021.

[27] Zarei, Seyed Fariborz, and Mostafa Parniani. "A comprehensive digital protection scheme for low-voltage microgrids with inverter-based and conventional distributed generations." IEEE Transactions on Power Delivery 32.1 (2016): 441-452.

[28] W. H. Kersting, Distribution System Modeling and Analysis, Boca Raton, FL: CRC, 2002.

[29] A. Gopi and P. A. D. V. Raj, "Distributed generation for line loss reduction in radial distribution system" proc.- ICETEEEM 2012, Int. Conf.Emerg. Trends Electr.Eng. Energy Manag., pp. 29-32,2012.

[30] Kawambwa, S., Mwifunyi, R., Mnyanghwalo, D. et al. An improved backward/forward sweep power flow method based on network tree depth for radial distribution systems. Journal of Electrical Systems and Inf Technol 8, 7 (2021). https://doi.org/10.1186/s43067-021-00031-0

[31] Mathworks Matlab. Natick, MA, 2009. [Online]. Available: http://www.mathworks.com

Morteza Behbahanipour received his BSc degree from Qom University of Technology, Qom, Iran, in 2017. He is currently pursuing his M.S. degree at the same university. His research interests focus on the application of power electronics in power distribution systems. His thesis is centered on fault location in active distribution networks with high penetration of inverter-based distributed generators.

Seyed Fariborz Zarei received his B.Sc. degree in Electrical Engineering from the Department of Electrical Engineering at Amirkabir University of Technology (Tehran Polytechnic), Tehran, Iran, in 2012. He continued his academic pursuits by achieving both his M.Sc. and Ph.D. degrees in Electrical Engineering from the Department of Electrical Engineering at Sharif University of Technology, Tehran, Iran, in 2014 and 2019, respectively. From February to August 2018, he served as a Visiting Ph.D. Scholar at the Department of Energy, Aalborg University, Aalborg, Denmark. In January 2021, Dr. Zarei joined Qom University of Technology, Qom, Iran, as an Assistant Professor in the Department of Electrical and Computer Engineering. Dr. Zarei has authored over 30 conference and journal papers in the field of power electronics and electrical power engineering. His research is centered on the application of power electronics systems in power grids, with a focus on modeling, control, protection, and stability aspects. Additionally, Dr. Zarei established the Power Electronic and Grid Laboratory at Qom University of Technology in January 2022. This laboratory conducts studies on DC/AC converters and their interaction with the AC power grid. The experimental platform of the laboratory offers a flexible environment for implementing diverse control methodologies on three-phase converters, facilitating investigations into control, protection, and stability aspects.

Mohammadhadi Shateri (Member, IEEE) received the B.Sc. degree (Hons.) in electrical engineering from the Amirkabir University of Technology (Tehran Polytechnic), Tehran, Iran, in 2012, the M.Sc. degree (Hons.) in electrical engineering from the University of Manitoba, Winnipeg, MB, Canada, in 2017, and the Ph.D. degree in electrical engineering from McGill University, Montreal, QC, Canada, in 2021. He is currently an Assistant Professor at École de technologie supérieure and a member of the Laboratoire d'imagerie, de vision et d'intelligence artificielle (LIVIA). His research interests include machine learning, data privacy, and security in machine learning models with a focus on deep generative models.